https://doi.org/10.5194/egusphere-2023-702
Preprint. Discussion started: 4 October 2023


**Measurement report:**

# Intra-annual Variability of Black/Brown Carbon and Its Interrelation with Meteorological Conditions over Gangtok, Sikkim

Pramod Kumar[1], Khushboo Sharma[1], Ankita Malu[2], Rajeev Rajak[2], Aparna Gupta[1], Bidyutjyoti Baruah[1], Shailesh Yadav[1], Thupstan Angchuk[1], Jayant Sharma[1], Rakesh Kumar Ranjan[1#], Anil Kumar Misra[1], and Nishchal Wanjari[1]

[1]DST's Centre of excellence on Water Resources, Cryosphere and Climate Change Studies, Department of Geology, Sikkim University, Gangtok, Sikkim, India -737102

[2]Department of Geology, Sikkim University, Gangtok, Sikkim, India -737102

[#]Corresponding Author: rkranjan@cus.ac.in

## Abstract

Black carbon (BC) and brown carbon (BrC) have versatile nature, and they have apparent role in the climate variability and changes. As the anthropogenic activity is surging, the BC and BrC are also reportedly increasing. So, the monitoring of BC/BrC and observation of land use land cover changes (LULCC) at regional level are necessary for the various interconnected meteorological phenomenal changes. The current study investigates BC, BrC, $CO_2$, BC from fossil fuels (BCff), BC from biomass burning (BCbb), LULCC, and their relationship to the corresponding meteorological conditions over Gangtok in Sikkim Himalayan region. The concentration of BC (BrC) 43.5 $\mu g/m^3$ (32.0 $\mu g/m^3$) is found to be highest during the March-2022 (April-2021). Surface pressure has been found to have a significant positive correlation with BC, BCff, BCbb and BrC. The boundary layer is calmer and more stable when the surface pressure is higher, which keeps contaminants deposited there. The wind, on the other hand, appears to represent the dispersion of pollutants with a strong negative correlation. The fact that all pollutants and precipitation have been shown to behave similarly points to moist scavenging of the pollutants. Despite the dense cloud cover, it is clear that the area is not receiving convective precipitation, implying that orographic precipitation is occurring over the region. Most of Sikkim receives convective rain from May to September, indicating that the region has significant convective activity contributed from the Bay of Bengal during monsoon season. Furthermore, monsoon months have the lowest concentrations of BC, BCbb, BCff, and BrC, suggesting the potential of convective rain (as rain out scavenging) to remove most of the pollutants. Moreover, BC and BrC show positive radiative feedback.

***Key words:*** Black carbon; Brown carbon; LULC; Sikkim Himalaya; Meteorology; Biomass burning; Radiative forcing.

https://doi.org/10.5194/egusphere-2023-702
Preprint. Discussion started: 4 October 2023


## 1.0 Introduction

Black carbon (BC), and brown carbon (BrC), are part of fine particulates air pollution that have apparent role in the climate variability and changes. BC/BrC is a short-lived climate pollutant with a lifetime of only days to weeks after release in the atmosphere (Pierrehumbert, 2014). During this short period of time, BC/BrC can have significant direct and indirect impacts on the climate, cryosphere, agriculture, and human health (Shindell et al., 2012). It consists of pure carbon in several interconnected forms. BC is formed through the incomplete combustion of fossil fuels, biofuel, and biomass, and is one of the main types of particles in both anthropogenic and naturally occurring soot (Bond et al., 2004). BrC in the atmosphere have been attributed to burning of biomass and fossil fuels, biogenic release of fungi, plant debris, and humic matter and multiphase reactions between the gas-phase, particulate, and cloud microdroplet constituents in the atmosphere (Laskin et al., 2015). BC/BrC is transported from its source to many locations across the world (Ramanathan and Carmichael, 2008). The released BC/BrC is vertically distributed and travels through the atmosphere according to wind speed and direction, interacting with numerous components before sinking on the earth's surface through wet or dry deposition. Its hygroscopic nature makes more susceptible to cloud seeding and cloud formation process and so directly helps in precipitation mechanism in high humid conditions (Stevens and Feingold, 2009). In addition, it absorbs both incoming and outgoing radiation, atmospheric BC/BrC modifies radiative forcing, disturbs atmospheric stability, regional circulation and rainfall pattern, affects cloud albedo, material damage, reduces agricultural productivity, degrades ecosystem and affects human health (Zhang et al., 2013). However, due to an insufficiency of observations, BrC is one of the least understood and uncertain warming agents (Yue et al., 2022). Several studies have been carried out to examine the concentration of BC and BrC all over the world and in India as well (Reddy and Venkataraman, 2002a, 2002b; Venkataraman et al., 2006; Park et al., 2010; Sloss, 2012; Helin et al., 2021; 2020; Kumar et al., 2020; Watham et al., 2021; Bhat et al., 2022; Runa et al., 2022; Yue et al., 2022; Kumar et al, 2018b). However, the overall worldwide BC emission is estimated to be 4800-7200 Gg per year (Klimont et al., 2017). In 2001, India's total BC emissions were projected to be 1343.78 Gg (Sloss, 2012). Residential fuel burning and transportation contributes maximum to the global anthropogenic BC emission (Helin et al., 2021). About 60 to 80% of residential fuels (coal and biomass) emissions are reported from Asian and African countries, whereas approximately 70% of diesel engines emission is found to be from Europe, North America, and Latin America.

https://doi.org/10.5194/egusphere-2023-702
Preprint. Discussion started: 4 October 2023


On the other hand, emissions on the Indian subcontinent have increased by 40% since the year of 2000. According to Reddy and Venkataraman (2002a, 2002b), the estimated BC emissions in India are fossil fuels, 100 Gg biofuel, 207 Gg open burning, and 39 Gg with a climatic forcing of +1.1 W/m$^2$, black carbon is the second-most significant human emission in the current atmosphere (Sharma et al., 2022). BC concentration was measured by Zhao et al. (2017) in the south-eastern Tibetan Plateau (TP). Daily mean BC loadings ranged from 57.7 to 5368.9 ng/m$^3$ demonstrating a high BC burden even at free tropospheric altitudes (Zhao et al., 2017). Black carbon (BC) deposition was estimated at the Nepal Climate Observatory - Pyramid (NCO-P) site in the Himalayan region during the pre-monsoon season (March-May). A total BC deposition rate of 2.89 µg/m$^3$/day was estimated, resulting in a total deposition of 266 µg/m$^3$ for March–May (Yasunari et al., 2010). From the Indian perspective, several key short-term incidents contribute to a rise in India's BC concentration from biomass burning and other sources (Kumar et al., 2020). Burning agricultural waste (stubble) is widespread in India and several other nations. Many studies suggest increased BC in northern India, notably Indo-Gangetic plain (IGP) is the global absorbing aerosol hotspot (Venkataraman et al., 2006; Ramanathan and Carmichael, 2008). In India post-monsoon paddy crop waste burning occurs in the month October and November in north and northwest part of India (Venkataraman et al., 2006). In the north-western Indo-Gangetic Plain (IGP) (especially- Punjab, Haryana, and western Uttar Pradesh), stubble burning is a popular practice (Venkataraman et al., 2006). Long-distance transport of BC aerosols, mostly from Asia to the north Pacific and South America to the southwest Atlantic, is often recognised as a significant factor in local concentration (Evangelista et al., 2007). However, in India only local sources (89%) affects BC concentrations (Zhang et al., 2013), as there aren't many movements of transboundary aerosols contribution over the IGP (Kumar et al., 2018a; Kedia et at., 2014; Ramachandran and Rupakheti, 2022; Ramachandran et al., 2020). Both marine and continental air masses contributed to total aerosol loading over middle-IGP (Kumar et al., 2017; Shukla et al., 2022).

Black carbon is a light-absorbing particle that are released into the atmosphere directly in the form of ultrafine (<0.1 µm) to fine particles (<2.5µm) (Gupta et al., 2017). BC is a good tracer for particle deposition as it is non-volatile, insoluble, and chemically inert, and it can also mix well with other aerosol species in the atmosphere (Kiran et al., 2018). As a result, BC deposition data are important not just for BC sinks but also for a broader understanding of aerosol deposition. BC emissions are mostly influenced by significant changes in the energy sector, fuel usage, industrial expansion, and an increase in the number of vehicles (Bisht et al., 2015). Residential fuel like wood, agricultural waste, and cow dung used for cooking and

https://doi.org/10.5194/egusphere-2023-702
Preprint. Discussion started: 4 October 2023


biomass usage for home purposes are the primary sources of BC emissions (Venkataraman et al., 2006). The Asian mainland is a substantial contributor to global BC emissions and has been identified as a hotspot (Gupta et al., 2017). BC has a high absorption ability, accounting for 90-95 percent of total atmospheric aerosol absorption (Hansen et al., 1984). It can absorb solar energy in the visible-infrared band and warm the environment. In comparison to carbon dioxide, BC has a much shorter life cycle in the atmosphere. As a result, mitigation or reduction has a greater positive impact on the atmosphere (Kirchstetter et al., 2004; Takemura and Suzuki, 2019). Changing land use land cover (LULC) has very significant impact on weather, climate and aerosols (Mahmood et al., 2010). It is well stabilised fact that the LULC change has direct relation with land surface temperature, vehicular emission and anthropogenic activity (Aithal and MC, 2019). Which motivated the present study for the further analysis for Sikkim region land use land cover change and its relation with temperature and BC/BrC for the March 2021 to March 2022. The current study's objectives are to assess the intra-annual variability of Black/Brown Carbon (BC/BrC) (diurnal/daily/monthly) during the study period March-2021 to March-2022, as well as the interrelationship between meteorological conditions and BC/BrC, along with LULC change for three decades 2000, 2010, and 2020, and its relationship with anthropogenic activity over Gangtok.

## 2.0 Study location

The Gangtok Municipal Corporation (GMC) has been selected for the present study on the basis of its urban exposer and settlement change for three decades as well as congruently temperature rise (figure S1). The sampling has been carried out at Pani House area in Gangtok, GMC, having longitude 88.609°E and latitude 27.323°N. Sikkim is surrounded by Nepal, China and Bhutan from west, north and east respectively and consists of the trans and greater Himalayan range. It has one of the most fragile forest covers. The Gangtok is densely populated city and capital of state Sikkim which is situated in the East Sikkim district (see figure 1a). The population of the Sikkim has been found to be increased as per Indian census for three decades as this can be seen in table S1.

## 3.0 Data and Methodology

The real time sampling of BC was carried out from 10$^{th}$ March 2021 to 17$^{th}$ March 2022, at Gangtok using the seven-channels dual spot Aethalometer (Model AE-33-7, Magee Scientific, USA). The data was collected for the measurement of BC and BrC associated with particulate matter having an aerodynamic diameter less than 2.5 µm ($PM_{2.5}$). The concentration of BC, BrC, BCbb, and BCff have been estimated by Carbonaceous Aerosol Analysis Tools (CAAT) software tool from the Magee Scientific Aethalometer model AE33 (Hansen and Schnell, 2005). The carbon dioxide ($CO_2$) was measured using a $CO_2$ sensor (Vaisala-GMP343) which is attached to the aethalometer. The inlet of the aethalometer was mounted at a height of 15 m above ground level. One of the main sources of uncertainty in using aerosol absorption measurements to estimate BrC mass concentration is the fact that other species, such as black carbon and dust, can also contribute to the measured absorption. This can lead to overestimation of BrC mass concentration, particularly in environments where these species are also present. However, in the Sikkim region has one of the higher precipitation regions in the world and negligible contribution of the dust pollution. Furthermore, there must be lesser over/under estimation. Therefore, the present study used mass concentration.

A new data set of BC, BrC, Black Carbon from biomass burning (BCbb), Black Carbon from fossil fuels (BCff), BrC, percentage contribution of biomass burning to BC (BB%) and $CO_2$ has been generated over the unreported region of Sikkim Himalaya. The diurnal and monthly data set of BC, BCbb, BCff, BrC, BB% and $CO_2$ have been given in the details in supplementary materials (Table S2 and S3). In addition to this the meteorological data has been selected ERA5 reanalysis for the study. LULC data has been taken from USGS earth explorer of 2000 and 2010 landsat-5, 2020 landsat-8, and 2021 for sentinel-2 (Karra et al., 2021). LULC data has been chosen for the month of December to minimize the cloud cover. The details of the LULC calculation steps used are given in the supplementary section (methodology S1.3). The brief of the data set is discussed in the table 1.

### 3.1 Estimation of BrC

The Carbonaceous Aerosol Analysis Tools (CAAT) software tool from the Magee Scientific Aethalometer model AE33 was utilized to estimate the concentrations of BC, BrC, BCbb, and BCff. The absorption coefficients of BC and BrC were determined using the multi-wavelength absorption coefficients provided by the aethalometer. The presence of BrC was identified by observing the maximum light absorption between 370–590 nm, but its absorption may increase significantly below this range depending on its composition. The attenuation of illumination measured in this study using the aethalometer was attributed solely to the contribution of BC and BrC. It is believed that the absorption coefficient at 370 nm measured by the aethalometer represents the combined absorption coefficients of BC and BrC, which is denoted as $\sigma$BC + BrC (370 nm). This assumption is similar to the model used in the multi-wavelength absorbance analyzer (MWAA) approach for source allocation, as described in Massabò et al. (2015). Equation (3.13) was used to calculate the $\sigma$BrC (370 nm) absorption coefficient

https://doi.org/10.5194/egusphere-2023-702
Preprint. Discussion started: 4 October 2023


(supplementary methodology S1), which involved subtracting the contribution of BC (σBC (370 nm)) from the observed absorption coefficient (σBC + BrC (370 nm)).

$$\sigma \text{BrC}(370\text{nm}) = \sigma \text{BC} + \text{BrC}(370 \text{ nm}) - \sigma \text{BC}(370 \text{ nm}) \qquad \text{Eq. (1)}$$

The σBC (370 nm), was calculated by applying the power-law fit to absorption data in the 590-950 nm wavelength range provided in equation (1).

$$\sigma \text{BC}(\lambda) = \beta \, \lambda^{-AAE} \text{BC} \qquad \text{Eq. (2)}$$

The absorption angstrom exponent of BC is denoted as $AAE_{BC}$, with β being a constant value. As BC is a significant contributor to light absorption at wavelengths beyond 590 nm, the contribution of other aerosol species can be neglected, and the $AAE_{BC}$ can be calculated using equation (3.15) (supplementary methodology S1), as stated in Rathod and Sahu (2022). The AAE for both BC and BrC can be expressed as σ, and in this study, the AAE definition by Moosmüller et al. (2011a) was used instead of the AAE specified for a wavelength pair. This value is determined by equation (2), which calculates the negative log-log slope of the absorption spectrum at wavelength λ.

$$\text{AAE} = \frac{dln\sigma \text{BC}}{d \ln\lambda} \qquad \text{Eq. (3)}$$

Instead of the conventional approach where AAEBC is assumed to be 1, we utilized the AAEBC that was observed onsite to calculate σBC(λ). Equation (3.16) was employed to determine σBrC (370 nm) by substituting σBC(λ) at 370 nm, which was obtained using equation (3), into equation (3.13) (refer to supplementary methodology S1.1, S1.2, and figure S2 for details).

$$\text{BrC}(370 \text{ nm}) = \text{BC} + \text{BrC}(370 \text{ nm}) - (370\text{nm}) - AAE_{BC} \qquad \text{Eq. (4)}$$

To calculate σBrC(λ) at 470 nm and 520 nm, we can subtract the modelled BC from the measured absorption coefficients, in a similar manner. It is worth noting that the BrC absorption coefficients are very low at wavelengths beyond 590 nm, according to Rathod et al. (2017) and Rathod and Sahu (2022), hence they are not taken into account (supplementary methodology S1).

### 3.2 Data Analysis

LULC change also has a direct impact on vehicular emissions and other anthropogenic activities. Urbanization, conceivably, can lead to increased vehicle traffic and emissions, which can contribute to air pollution and climate change. Changes in land use can also affect the amount and type of vegetation, which can influence the carbon cycle and the amount of greenhouse gases in the atmosphere. The ERA-5 reanalysis data has been used for meteorological analysis viz. wind pattern, precipitation, relative humidity, and temperature (Hersbach et al., 2020). The hourly data has been taken for the analysis and then daily, monthly and seasonal average has been computed for the study period over the Sikkim and surrounding states for a better understanding the meteorological conditions influencing the BC, and BrC. The total precipitation is computed as sum of the hourly data for a day to daily total precipitation and further it was summed for monthly cumulative total precipitation using sum formula as

$$\text{Monthly Cumulative Total Precipitation} = \sum_i^n X \qquad \text{Eq. (5)}$$

Where, 'i' is the initial and 'n' the last date and X is hourly total precipitation taken from ERA5. The wind circulation has been computed using u-component and v-component of wind and the wind speed has been calculate as

$$\text{Wind Speed} = \sqrt{u^2 + v^2} \qquad \text{Eq. (6)}$$

The temperature and relative humidity averaged have been computed using mean formula as

$$Average = \frac{\sum_i^n X}{n} \qquad \text{Eq. (7)}$$

Where, 'i' is initial and 'n' last date of the of variables such as temperature, relative humidity and wind components.

Let x and y be two real-valued random variables such that the correlation coefficient spearmen Pearson can be calculated between the BC/BrC and meteorological parameters. The Coefficient of Pearson Correlation (PCC) (Pearson, 1909; Benesty et al., 2009) as

$$PCC = \frac{n(\sum xy) - (\sum x)(\sum y)}{\sqrt{[n\sum x^2 - (\sum x)^2][n\sum y^2 - (\sum y)^2]}} \qquad \text{Eq. (8)}$$

Where 'n' is the population size of the variables used for the study.

Table 1 contains additional information about the dataset, and a more detailed methodology can be found in the supplementary section (S1).

## 4.0 Results and Discussions

The anthropogenic activities in Gangtok are drastically increased in last 20 years. As evident from figure 1b, c and d, LULC has been changed since 2000 to 2020 over the Gangtok

https://doi.org/10.5194/egusphere-2023-702
Preprint. Discussion started: 4 October 2023


municipal corporation (GMC). The population change and growth have also been observed over the Sikkim (Table S1). LULC during year 2000 and 2010 evidently shows that most of the fallow land has been built-up due to recent change in the policy of construction in Sikkim suggesting urban settlement load over Gangtok is increased significantly. As a result, there is a significant increase in built-up areas in GMC for last 20years. The vegetation cover has also reduced since 2000 to 2020 (figure 1b, c, and d). The rainfed water bodies are reducing from the GMC. However, due to its seasonal nature, streams are lesser emerged in 2020. Which perhaps shows the precipitation pattern alteration over GMC due to highly built-up sprawl. The built-up extent has been sprawling and consuming the dense vegetation regions as well. This increases the study region's urge to be acknowledged so that Sikkim's future policymakers can consider the effects of rising anthropogenic activities. This anthropogenic activity leading to heavy load on environmental over one of the cleanest states of India. Long-term spatiotemporal variation of 2-meter air temperature justifies the LULC change and warming pattern over the Gangtok region (figure S1a, S1b, S1c, S1d, and S1e). The decadal warming rate is varying from 0.25$^{O}$ to 0.45$^{O}$C (figure S1e). Thereafter, BC and BrC over the Gangtok has been measured to report the issue and get more attention to the scientific and local community. The higher anthropogenic activity releases the higher amount of emission in the name of development due to population load on the region (i.e., growth rate has been raised from 12.89 to 13.05% in recent years) (Table S11). Diurnal variation of the BC, BrC, BC BCbb, BC BCff and $CO_2$ apparently show two peaks. BC, BCff and $CO_2$ have almost similar time of peaks observed. The first peak is found during 8-10AM. And, the second peak is observed during 8-10PM. However, BrC and BCbb have the peak concentration during 10-11AM (figure 2a). The same for meteorological conditions is observed and referred to figure 2b.

The daily timeseries of the BC, BCbb, BCff, BrC, BB% and $CO_2$ show the highest fluctuation during 20$^{th}$ to 30$^{th}$ March in both 2021 and 2022 years respectively. The maximum BC (BrC) content was found in March 2022 (April-2021), at 43.5µg/m$^3$ (32µg/m$^3$). The lowest fluctuation is observed during 15$^{th}$ May to 15$^{th}$ September 2021 (figure 3a). The intense peaks of BC, BCff and $CO_2$ has been observed during 10$^{th}$ October to 15$^{th}$ November 2021 (figure 3a) that may be linked to the heavy tourist season of the state and indicating towards the traffic overload in the Gangtok (Sharma et al, 2022). As, the meteorological conditions are also favouring the similar circumstances to accumulate the pollutant during 10$^{th}$ October to 15$^{th}$ November 2021 (figure 3b). The lowest surface pressure with minimum fluctuation and the highest temperature and dewpoint temperature with minimum fluctuation is being noticed

https://doi.org/10.5194/egusphere-2023-702
Preprint. Discussion started: 4 October 2023


during the 15th June to 20th September 2021 (figure 3b). BrC is found the highest with maximum fluctuation during 10th January to 30th March that is pointing towards winter wood burning for the subsistence as similar observed BCbb. The monthly variations of BC, BCbb, BCff, BrC, BB% is discussed in figure 4a, and the highest value of standard deviation were observed during March 2022 for BC, BCff, and April 2021 for BCbb, BrC, BB%. The $CO_2$ is observed almost constant with a small value of standard deviation. The maximum concentration of the BC, BCff is found in March 2022. However, BCbb and BrC were measured highest in April 2021. The minimum concentration of the BrC was seen in the month of August 2021 as the highest total precipitation month with high wind speed, temperature and dewpoint temperature and relative humidity (figure 4b, S3 and S4).

The good significant correlation between BC and BCff suggested that the major contribution of the BC is fossil fuel burning (Osborne et al, 2008). A strong significant correlation between BCbb and BrC indicating that major contributor of BrC is biomass burning that can be justified by BB% and BrC strong significant positive correlation coefficient (figure 5). A good significant positive correlation between $CO_2$ and BC/BCff suggesting that fossil fuel burning is one of the causes of $CO_2$ concentration or vis versa. Dewpoint temperature and $CO_2$ has strong significant positive correlation coefficient suggesting to positive radiative forcing of the $CO_2$. The Similar has been found for the temperature. BCbb/BrC and temperature has strong significant negative correlation suggesting the negative radiative nature of the BCbb/BrC (figure S5). Moreover, net thermal/solar radiation (STR/SSR) and BC/BrC have significant positive correlation (figure 5, and S5). A strong significant positive correlation between surface pressure and BC/BCff (BCbb/BrC) has been observed (figure 5). Higher the surface pressure makes calm condition and stable boundary layer, which keeps the pollutants accumulated in the boundary layer (Bharali et al., 2019). However, the opposite has been observed for the wind that indicates the dispersion of pollutants with strong negative correlation. The similar has been observed for the total precipitation and all the pollutants, delineates to wet scavenging of the pollutants. The relative humidity is also showing the similar result to the total precipitation with greater values of coefficient. The negative correlation between total precipitation and surface pressure suggested that the rain fall over the region mostly occurs in low pressure system that is causes due to the vertical rising of air parcel and cause to condensation and precipitation. However, cloud condensation nuclei formation and precipitation are prompted by aerosols (BC and BrC). Thereafter, BC and BrC have crucial role in precipitation mechanism.

https://doi.org/10.5194/egusphere-2023-702
Preprint. Discussion started: 4 October 2023


Total precipitation and wind circulation suggested that the study region is receiving precipitation in entire month of the study period (i. e., most of the time rain form and sometimes snow). As the maxima is observed during the month of August and minima during March 2022. The wind pattern delineates during the May to September 2021 the monsoon seasonal strong effect (figure 6). And rest of the period the wind is conversing in the valley and diverging from the mountain (figure 6). The strong wind and heavy rain fall suggested the pollutant scavenging (rain out or wash out) that is why it is significant negatively correlated. The relative humidity and temperature patten also justify the same as the temperature gradients change from January to December and moisture content reduction in the atmosphere (figure S6). The lowest in month of February is observed and temperature gradient getting steep from the November (figure S6). The dewpoint temperature contour and surface pressure shading match well suggesting that the surface pressure creates the dewpoint temperature gradient and keep it sustained and stable atmospheric condition (figure S7). During month of June, it is very peculiar that the dewpoint temperature contours are wide and very small gradient is observed (figure 7). Which is pointing toward the warm condition during the June over entire Sikkim. Figure 7 discusses about the cloud cover and convective precipitation over the Sikkim. It is clear from (figure 7a to d) the region is not receiving the much convective precipitation even if there is huge cloud cover, which leads to a conclusion of orographic precipitation over the region (figure 7). However, the relative humidity is very high over the sampling site from lower to upper middle level of the atmosphere during the study period (figure S3). During May to September the convective rain is receiving most part of the Sikkim approved that the region has high convective activity added from the Bay of Bengal as the monsoon season. Again, from October to April the region is not receiving the convective rain even though there is strong cloud cover pointing toward the orographic rainfall over entire Sikkim. That's making the Sikkim unique weather condition (figure S3 and S4). And, least concentration of BC, BCff, BCbb and BrC is observed during the monsoon months supporting the convective rain (i.e., rain out scavenging) of all pollutants. The BC and BrC have a significant positive correlation with thermal and solar radiation, indicating positive radiative feedback. A stronger negative correlation between CO2 and surface thermal radiation (STR) and surface solar radiation (SSR) would have significant implications (figure 5). The negative correlation between CO2 and STR implies that as the concentration of CO2 in the atmosphere increases, the amount of heat radiated from the Earth's surface into space decreases. This can lead to an increase in the Gangtok's temperature, which can have various impacts on climate and weather as well (figure S1, and 5). The negative correlation between CO2 and SSR implies that as the concentration

https://doi.org/10.5194/egusphere-2023-702
Preprint. Discussion started: 4 October 2023


of CO2 in the atmosphere increases, the amount of solar radiation absorbed by the Earth's surface decreases (figure 5). Overall, a significant negative correlation between CO2 and STR/SSR would indicate a stronger influence of greenhouse gas concentrations on the surface's radiation balance and would have important implications for climate change as well as anomalous warming over the Gangtok region (figure S1).

## 5.0 Conclusions

In accordance with the LULC between 2000 and 2010, Sikkim's recent changes to its development regulations have resulted in the majority of fallow land being consumed by construction, which suggests that Gangtok's urban settlement load has increased significantly. In addition, the LULC for 2020 depicts a booming built-up region over the GMC. Since 2000 to 2020, the vegetation cover has likewise decreased. However, due to the seasonal nature, streams are lesser in 2020, indicating precipitation pattern variation over GMC. The areas covered in dense vegetation are also being consumed by the expanding built-up area. The present study is the report of newly produced data BC and BrC for the fragile region of Himalayas and relation with meteorological conditions. It has been observed that the temperature over Gangtok is increasing as well. The peak concentration of BC/BrC has been found during October 2021 and March 2021 and 2022. The diurnal distribution of BC/BrC suggests the two peaks in a day, first in the 8-10AM and second in 9-11PM. The meteorological conditions for the same has been observed to be favourable to diurnal variation of BC/BrC concentration. In the monthly variation of the BC/BrC is delineated that the peak concentration of BC, BCbb, BCff, during March 2022. However, BrC and BB% have maximum concentration during April 2021. BB% and BrC as well as BB and carbon dioxide have a strong significant positive correlation coefficient, which is evidence that biomass burning is a substantial factor in the rise in carbon dioxide levels. In addition to this, there is a strong, positive correlation between $CO_2$ and BC/BCff, indicating that burning fossil fuels is also one of the causes of rising $CO_2$ levels. The net thermal radiation, net solar radiation and BC, BrC relationship suggested that the BC, and BrC have positive radiative forcing. Furthermore, the monsoon months show the lowest concentrations of BC, BCbb, BCff, BrC, and BB%, demonstrating the convective rain (i.e., rain out scavenging) ability to remove majority of contaminants. Both the BC and BrC reveal evidence of positive radiative feedback.

## Data Availability

Data is provided in the ‘supplementary section’ and for further detail knowledge about it can be available from the corresponding author on the adequate request.

Data link for the data access:
https://docs.google.com/spreadsheets/d/1N4F_fT68syY6n0UIfA6nzI5o-8LUWjyFfk5NpfquRyg/edit?usp=sharing

**Conflict of Interest**

None conflict of interest.

**Authors Contribution**

Dr. Pramod Kumar: conceptualization, drafting, writing, figures, and editing

Ms. Khushboo Sharma: sampling, data analysis and figures.

Ms. Ankita Malu: data analysis, figures, and editing

Mr. Rajeev Rajak: editing

Ms. Aparna Gupta: editing

Mr. Bidyutjyoti Baruah: editing

Mr. Jayant Sharma: sampling

Dr. Shailesh Yadav: editing, and mentoring

Dr. Thupstan Angchuk: editing, and mentoring

Dr. Rakesh Kumar Ranjan: conceptualization, data interpretation, mentoring, and editing.

Dr. Nishchal Wanjari: editing and mentoring.

Dr. Anil Kumar Misra: editing and mentoring.

**Acknowledgements**

Authors acknowledge to the Department of Science and Technology, Government of India, and host department "DST's Centre of Excellence (CoE), at Department of Geology, Sikkim University, DST/CCP/CoE/186/2019 (G)," for the generation of BC/BrC data. We also acknowledge to free data sources used in the study as ERA5, USGS earth explorer. Authors appreciate freely available software such as R-studio, QGIS, CDO, and GrADS used for the analysis and visualization. We also acknowledge the anonymous persons whom so ever have helped and supported for the Black Carbon data collection.

**References**

Aithal, B. H., & MC, C. (2019). Assessing land surface temperature and land use change through spatio-temporal analysis: a case study of select major cities of India. Arabian Journal of Geosciences, 12(11), 1-16. https://doi.org/10.1007/s12517-019-4547-1

Benesty, J., Chen, J., Huang, Y., and Cohen, I. (2009). Pearson correlation coefficient. In Noise reduction in speech processing (pp. 1-4). Springer, Berlin, Heidelberg. https://doi.org/10.1007/978-3-642-00296-0_5

Bharali, C., Nair, V. S., Chutia, L., & Babu, S. S. (2019). Modeling of the effects of wintertime aerosols on boundary layer properties over the Indo Gangetic Plain. Journal of Geophysical Research: Atmospheres, 124(7), 4141-4157. https://doi.org/10.1029/2018JD029758

Bhat, M. A., Romshoo, S. A., & Beig, G. (2022). Characteristics, source apportionment and long-range transport of black carbon at a high-altitude urban centre in the Kashmir valley, North-western Himalaya. Environmental Pollution, 305, 119295. https://doi.org/10.1016/j.envpol.2022.119295

Bisht, D.S., Dumka, U.C., Kaskaoutis, D.G., Pipal, A.S., Srivastava, A.K., Soni, V.K., Attri, S.D., Sateesh, M. and Tiwari, S., (2015). Carbonaceous aerosols and pollutants over Delhi urban environment: temporal evolution, source apportionment and radiative forcing. Science of the Total Environment, 521, 431-445. https://doi.org/10.1016/j.scitotenv.2015.03.083

Bond, T. C., Streets, D. G., Yarber, K. F., Nelson, S. M., Woo, J. H., & Klimont, Z. (2004). A technology-based global inventory of black and organic carbon emissions from combustion. Journal of Geophysical Research: Atmospheres, 109(D14). https://doi.org/10.1029/2003JD003697

Evangelista, H., Maldonado, J., Godoi, R.H.M., Pereira, E.B., Koch, D., Tanizaki-Fonseca, K., Van Grieken, R., Sampaio, M., Setzer, A., Alencar, A. and Gonçalves, S.C. (2007). Sources and transport of urban and biomass burning aerosol black carbon at the South–West Atlantic Coast. Journal of Atmospheric Chemistry, 56(3), 225-238. https://doi.org/10.1007/s10874-006-9052-8

Gupta, P., Singh, S. P., Jangid, A., & Kumar, R. (2017). Characterization of black carbon in the ambient air of Agra, India: Seasonal variation and meteorological influence. Advances in Atmospheric Sciences, 34(9), 1082-1094. https://doi.org/10.1007/s00376-017-6234-z

Hansen, A. D. A., & Schnell, R. C. (2005). The aethalometer. Magee Scientific Company, Berkeley, California, USA, 7.

Hansen, J., Lacis, A., Rind, D., Russell, G., Stone, P., Fung, I., Ruedy, R. and Lerner, J. (1984). Climate sensitivity: Analysis of feedback mechanisms. feedback, 1, 1-3.

Helin, A., Virkkula, A., Backman, J., Pirjola, L., Sippula, O., Aakko-Saksa, P., Väätäinen, S., Mylläri, F., Järvinen, A., Bloss, M. and Aurela, M. (2021). Variation of absorption Ångström exponent in aerosols from different emission sources. Journal of Geophysical Research: Atmospheres, 126(10), 2020JD034094. https://doi.org/10.1029/2020JD034094

Hersbach, H., Bell, B., Berrisford, P., Hirahara, S., Horányi, A., Muñoz-Sabater, J., Nicolas, J., Peubey, C., Radu, R., Schepers, D. and Simmons, A. (2020). The ERA5 global reanalysis. Quarterly Journal of the Royal Meteorological Society, 146(730), 1999-2049. https://doi.org/10.1002/qj.3803

Karra, K., Kontgis, C., Statman-Weil, Z., Mazzariello, J. C., Mathis, M., & Brumby, S. P. (2021). Global land use/land cover with Sentinel 2 and deep learning. In 2021 IEEE international geoscience and remote sensing symposium IGARSS (pp. 4704-4707). IEEE. https://doi.org/10.1109/IGARSS47720.2021.9553499

Kedia, S., Ramachandran, S., Holben, B. N., & Tripathi, S. N. (2014). Quantification of aerosol type, and sources of aerosols over the Indo-Gangetic Plain. Atmospheric Environment, 98, 607-619. https://doi.org/10.1016/j.atmosenv.2014.09.022

https://doi.org/10.5194/egusphere-2023-702
Preprint. Discussion started: 4 October 2023


Kirchstetter, T. W., Novakov, T., & Hobbs, P. V. (2004). Evidence that the spectral dependence of light absorption by aerosols is affected by organic carbon. Journal of Geophysical Research: Atmospheres, 109(D21). https://doi.org/10.1029/2004JD004999

Kiran, V. R., Talukdar, S., Ratnam, M. V., & Jayaraman, A. (2018). Long-term observations of black carbon aerosol over a rural location in southern peninsular India: Role of dynamics and meteorology. Atmospheric Environment, 189, 264-274. https://doi.org/10.1016/j.atmosenv.2018.06.020

Klimont, Z., Kupiainen, K., Heyes, C., Purohit, P., Cofala, J., Rafaj, P., Borken-Kleefeld, J. and Schöpp, W. (2017). Global anthropogenic emissions of particulate matter including black carbon. Atmospheric Chemistry and Physics, 17(14), 8681-8723. https://doi.org/10.5194/acp-17-8681-2017

Kumar, M., Parmar, K. S., Kumar, D. B., Mhawish, A., Broday, D. M., Mall, R. K., & Banerjee, T. (2018a). Long-term aerosol climatology over Indo-Gangetic Plain: Trend, prediction and potential source fields. Atmospheric environment, 180, 37-50. https://doi.org/10.1016/j.atmosenv.2018.02.027

Kumar, M., Raju, M. P., Singh, R. S., & Banerjee, T. (2017). Impact of drought and normal monsoon scenarios on aerosol induced radiative forcing and atmospheric heating in Varanasi over middle Indo-Gangetic Plain. Journal of Aerosol Science, 113, 95-107. https://doi.org/10.1016/j.jaerosci.2017.07.016

Kumar, P., Patton, A. P., Durant, J. L., & Frey, H. C. (2018b). A review of factors impacting exposure to PM2.5, ultrafine particles and black carbon in Asian transport microenvironments. Atmospheric environment, 187, 301-316. https://doi.org/10.1016/j.atmosenv.2018.05.046

Kumar, R. R., Soni, V. K., & Jain, M. K. (2020). Evaluation of spatial and temporal heterogeneity of black carbon aerosol mass concentration over India using three year measurements from IMD BC observation network. Science of the Total Environment, 723, 138060. https://doi.org/10.1016/j.scitotenv.2020.138060

Laskin, A., Laskin, J., & Nizkorodov, S. A. (2015). Chemistry of atmospheric brown carbon. Chemical reviews, 115(10), 4335-4382. https://doi.org/10.1021/cr5006167

Mahmood, R., Pielke Sr, R.A., Hubbard, K.G., Niyogi, D., Bonan, G., Lawrence, P., McNider, R., McAlpine, C., Etter, A., Gameda, S. and Qian, B. (2010). Impacts of land use/land cover change on climate and future research priorities. Bulletin of the American Meteorological Society, 91(1), 37-46. https://doi.org/10.1175/2009BAMS2769.1

Massabò, D., Caponi, L., Bernardoni, V., Bove, M.C., Brotto, P., Calzolai, G., Cassola, F., Chiari, M., Fedi, M.E., Fermo, P. and Giannoni, M. (2015). Multi-wavelength optical determination of black and brown carbon in atmospheric aerosols. Atmospheric Environment, 108,1-12. https://doi.org/10.1016/j.atmosenv.2015.02.058

Moosmüller, H., Chakrabarty, R. K., Ehlers, K. M., & Arnott, W. P. (2011a). Absorption Ångström coefficient, brown carbon, and aerosols: basic concepts, bulk matter, and spherical particles. Atmospheric Chemistry and Physics, 11(3), 1217-1225. https://doi.org/10.1021/acs.estlett.8b00118

Osborne, S. R., Johnson, B. T., Haywood, J. M., Baran, A. J., Harrison, M. A. J., & McConnell, C. L. (2008). Physical and optical properties of mineral dust aerosol during the Dust and

https://doi.org/10.5194/egusphere-2023-702
Preprint. Discussion started: 4 October 2023


Biomass-burning Experiment. Journal of Geophysical Research: Atmospheres, 113(D23). https://doi.org/10.1029/2007JD009551

Park, RJ, Kim, MJ, Jeong, JI, Youn, D., & Kim, S. (2010). A contribution of brown carbon aerosol to the aerosol light absorption and its radiative forcing in East Asia. Atmospheric Environment, 44 (11), 1414-1421. https://doi.org/10.1016/j.atmosenv.2010.01.042

Pearson, K. (1909). Determination of the coefficient of correlation. Science, 30(757), 23-25. DOI:10.1126/science.30.757.23

Pierrehumbert, R. T. (2014). Short-lived climate pollution. Annual Review of Earth and Planetary Sciences, 42, 341-379. DOI: 10.1146/annurev-earth-060313-054843

Ramachandran, S., & Rupakheti, M. (2022). Trends in the types and absorption characteristics of ambient aerosols over the Indo-Gangetic Plain and North China Plain in last two decades. Science of The Total Environment, 831, 154867. https://doi.org/10.1016/j.scitotenv.2022.154867

Ramachandran, S., Rupakheti, M., & Lawrence, M. G. (2020). Black carbon dominates the aerosol absorption over the Indo-Gangetic Plain and the Himalayan foothills. Environment international, 142, 105814. https://doi.org/10.1016/j.envint.2020.105814

Ramanathan, V., & Carmichael, G. (2008). Global and regional climate changes due to black carbon. Nature geoscience, 1(4), 221-227. https://doi.org/10.1038/ngeo156

Rathod, T. D., & Sahu, S. K. (2022). Measurements of optical properties of black and brown carbon using multi-wavelength absorption technique at Mumbai, India. Journal of Earth System Science, 131(1), 32. https://doi.org/10.1007/s12040-021-01774-0

Rathod, T., Sahu, S. K., Tiwari, M., Yousaf, A., Bhangare, R. C., & Pandit, G. G. (2017). Light absorbing properties of brown carbon generated from pyrolytic combustion of household biofuels. Aerosol and Air Quality Research, 17(1), 108-116. https://doi.org/10.4209/aaqr.2015.11.0639

Reddy, M. S., & Venkataraman, C. (2002a). Inventory of aerosol and sulphur dioxide emissions from India: I—Fossil fuel combustion. Atmospheric Environment, 36(4), 677-697. https://doi.org/10.1016/S1352-2310(01)00463-0

Reddy, M. S., & Venkataraman, C. (2002b). Inventory of aerosol and sulphur dioxide emissions from India. Part II—biomass combustion. Atmospheric Environment, 36(4), 699-712. https://doi.org/10.1016/S1352-2310(01)00464-2

Runa, F., Islam, M., Jeba, F., & Salam, A. (2022). Light absorption properties of brown carbon from biomass burning emissions. Environmental Science and Pollution Research, 29(14), 21012-21022. https://doi.org/10.1007/s11356-021-17220-z

Sharma, K., Ranjan, R.K., Lohar, S., Sharma, J., Rajak, R., Gupta, A., Prakash, A. and Pandey, A.K. (2022). Black Carbon Concentration during Spring Season at High Altitude Urban Center in Eastern Himalayan Region of India. Asian Journal of Atmospheric Environment (AJAE), 16(1). https://doi.org/10.5572/ajae.2021.149

Shindell, D., Kuylenstierna, J.C., Vignati, E., van Dingenen, R., Amann, M., Klimont, Z., Anenberg, S.C., Muller, N., Janssens-Maenhout, G., Raes, F. and Schwartz, J. (2012).

https://doi.org/10.5194/egusphere-2023-702
Preprint. Discussion started: 4 October 2023


Simultaneously mitigating near-term climate change and improving human health and food security. Science, 335(6065), 183-189. DOI: 10.1126/science.1210026

Shukla, K. K., Sarangi, C., Attada, R., & Kumar, P. (2022). Characteristic dissimilarities during high aerosol loading days between western and eastern Indo-Gangetic Plain. Atmospheric Environment, 269, 118837. https://doi.org/10.1016/j.atmosenv.2021.118837

Sloss, L. (2012). Black carbon emissions in India. CCC/209. IEA Clean Coal Centre, London, 38.

Stevens, B., & Feingold, G. (2009). Untangling aerosol effects on clouds and precipitation in a buffered system. Nature, 461(7264), 607-613. https://doi.org/10.1038/nature08281

Takemura, T., & Suzuki, K. (2019). Weak global warming mitigation by reducing black carbon emissions. Scientific reports, 9(1), 1-6. https://doi.org/10.1038/s41598-019-41181-6

Venkataraman, C., Habib, G., Kadamba, D., Shrivastava, M., Leon, J.F., Crouzille, B., Boucher, O. and Streets, D.G. (2006). Emissions from open biomass burning in India: Integrating the inventory approach with high-resolution Moderate Resolution Imaging Spectroradiometer (MODIS) active-fire and land cover data. Global biogeochemical cycles, 20(2). https://doi.org/10.1029/2005GB002547

Watham, T., Padalia, H., Srinet, R., Nandy, S., Verma, P. A., & Chauhan, P. (2021). Seasonal dynamics and impact factors of atmospheric CO2 concentration over subtropical forest canopies: observation from eddy covariance tower and OCO-2 satellite in Northwest Himalaya, India. Environmental Monitoring and Assessment, 193(2), 1-15. https://doi.org/10.1007/s10661-021-08896-4

Yasunari, T., Bonasoni, P., Laj, P., Fujita, K., Vuillermoz, E., Marinoni, A., Cristofanelli, P., Duchi, R., Tartari, G. and Lau, K.M. (2010). Estimated impact of black carbon deposition during pre-monsoon season from Nepal Climate Observatory–Pyramid data and snow albedo changes over Himalayan glaciers. Atmospheric Chemistry and Physics, 10(14), 6603-6615. https://doi.org/10.5194/acp-10-6603-2010

Yue, S., Zhu, J., Chen, S., Xie, Q., Li, W., Li, L., Ren, H., Su, S., Li, P., Ma, H. and Fan, Y. (2022). Brown carbon from biomass burning imposes strong circum-Arctic warming. One Earth, 5(3), 293-304. https://doi.org/10.1016/j.oneear.2022.02.006

Zhang, R., Jing, J., Tao, J., Hsu, S.-C., Wang, G., Cao, J., Lee, C. S. L., Zhu, L., Chen, Z., Zhao, Y., and Shen, Z. (2013). Chemical characterization and source apportionment of PM2.5 in Beijing: seasonal perspective, Atmos. Chem. Phys., 13, 7053–7074, https://doi.org/10.5194/acp-13-7053-2013

https://doi.org/10.5194/egusphere-2023-702
Preprint. Discussion started: 4 October 2023


## List of Figures

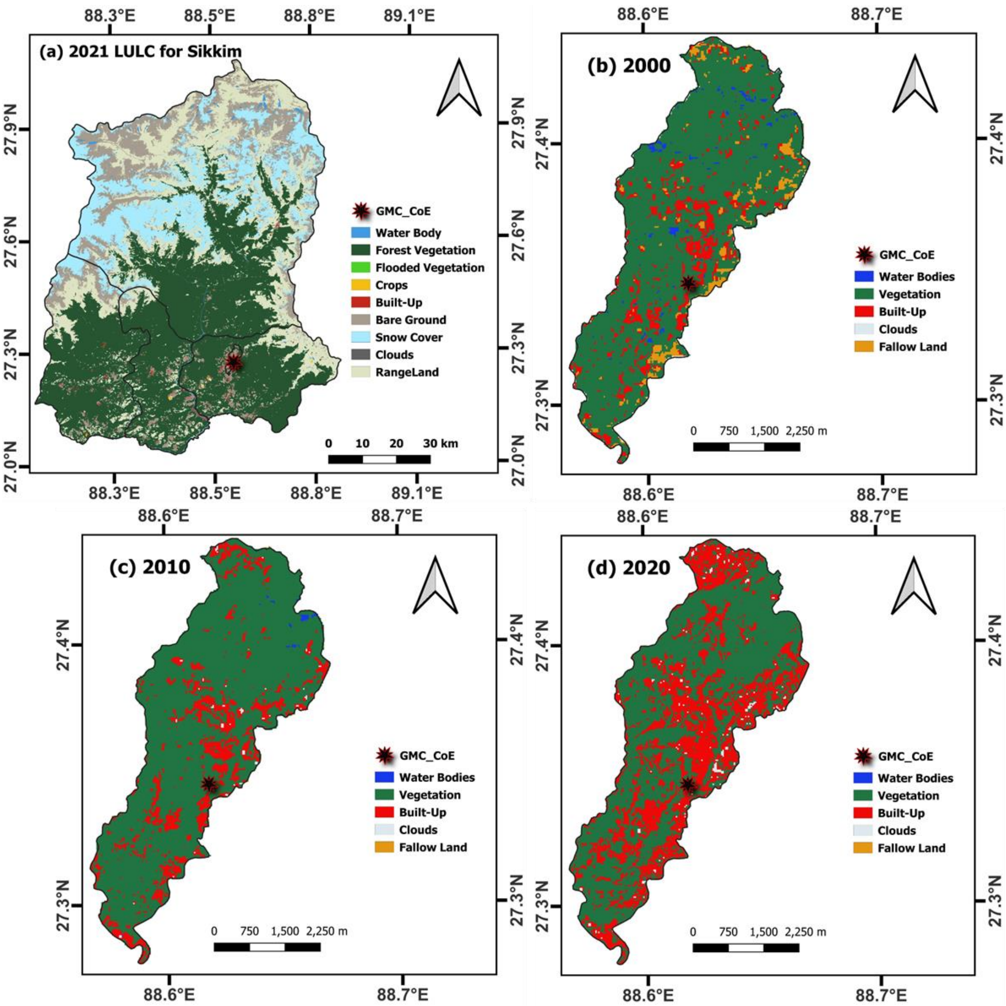


Figure 1. The study location and land use land cover for 2000, 2010, 2020, and 2021 for December over Gangtok and Sikkim region using landsat-5, landsat-8 and sentinel-2 data sets.

https://doi.org/10.5194/egusphere-2023-702
Preprint. Discussion started: 4 October 2023


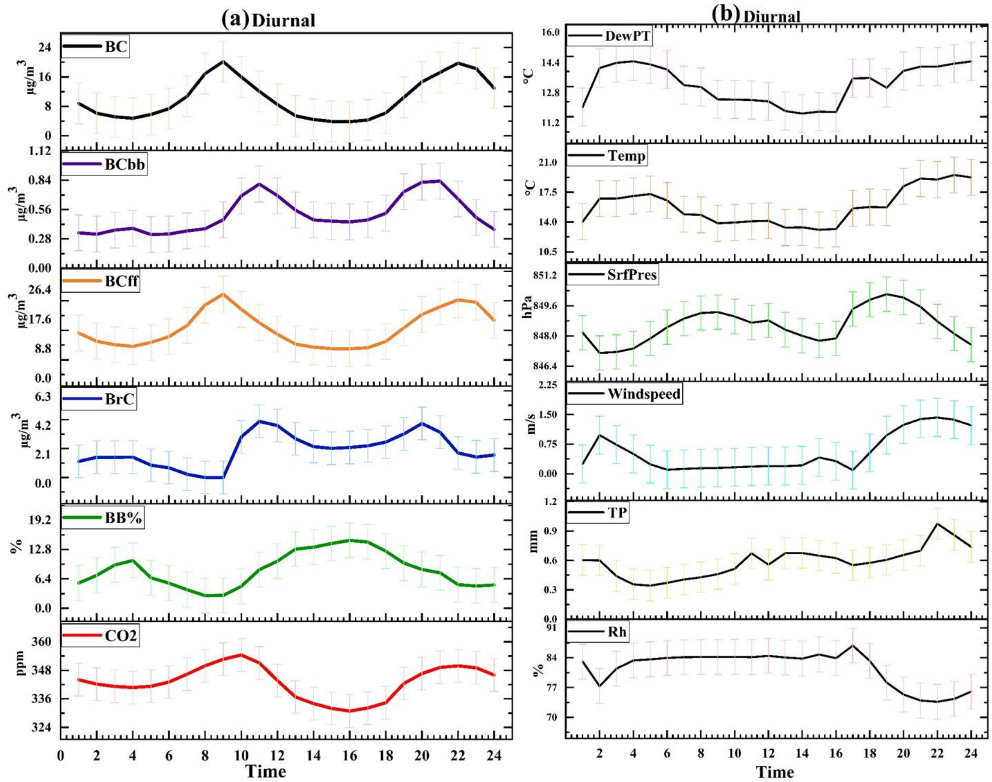


Figure 2. (a) The hourly observation of Black Carbon, Black Carbon through biomass burning, Black Carbon through fossil fuel, Brown Carbon, Biomass Burning percentage and Carbon Dioxide (BC, BCbb, BCff, BrC, BB%, and $CO_2$, respectively) (The corresponding unit for BC, BCbb, BCff, BrC: μg/m$^3$; BB%: % and $CO_2$: ppm) for 16$^{th}$ March 2021 to 10$^{th}$ March 2022 over study location (lat:27.32; lon:88.61). The light colour shading refers ±σ standard deviation for each variable. (b) Same as figure 2a, but for meteorological parameters as dewpoint temperature (DewPT), temperature (Temp), surface pressure (SrfPres), windspeed, total precipitation (TP), and relative humidity (Rh) during 16$^{th}$ March 2021 to 10$^{th}$ March 2022.

https://doi.org/10.5194/egusphere-2023-702
Preprint. Discussion started: 4 October 2023


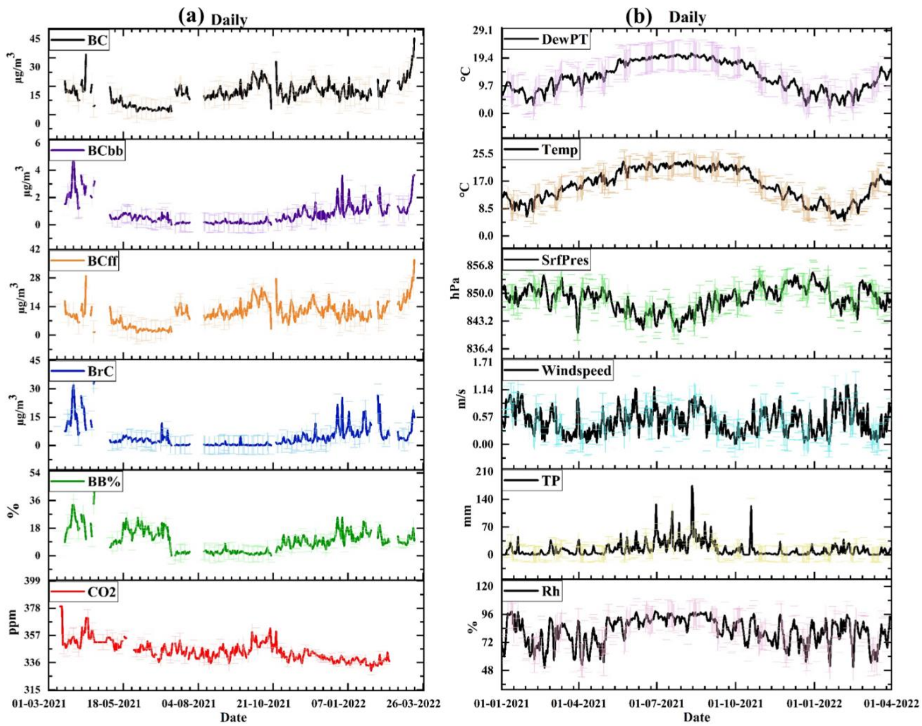


Figure 3. (a) The daily mean of Black Carbon, Black Carbon through biomass burning, Black Carbon through fossil fuel, Brown Carbon, Biomass Burning percentage and Carbon Dioxide (BC, BCbb, BCff, BrC, BB%, and $CO_2$, respectively) (The corresponding unit for BC, BCbb, BCff, BrC: µg/m3; BB%: % and $CO_2$: ppm) for 16$^{th}$ March 2021 to 10$^{th}$ March 2022 over study location (lat:27.32; lon:88.61). The light colour shading refers ±σ standard deviation for each variable. (b) same as figure 3a, but for meteorological parameters as dewpoint temperature (DewPT), temperature (Temp), surface pressure (SrfPres), Windspeed, total precipitation (TP), and relative humidity (Rh) during 1$^{st}$ January 2021 to 31$^{st}$ March 2022.

https://doi.org/10.5194/egusphere-2023-702
Preprint. Discussion started: 4 October 2023


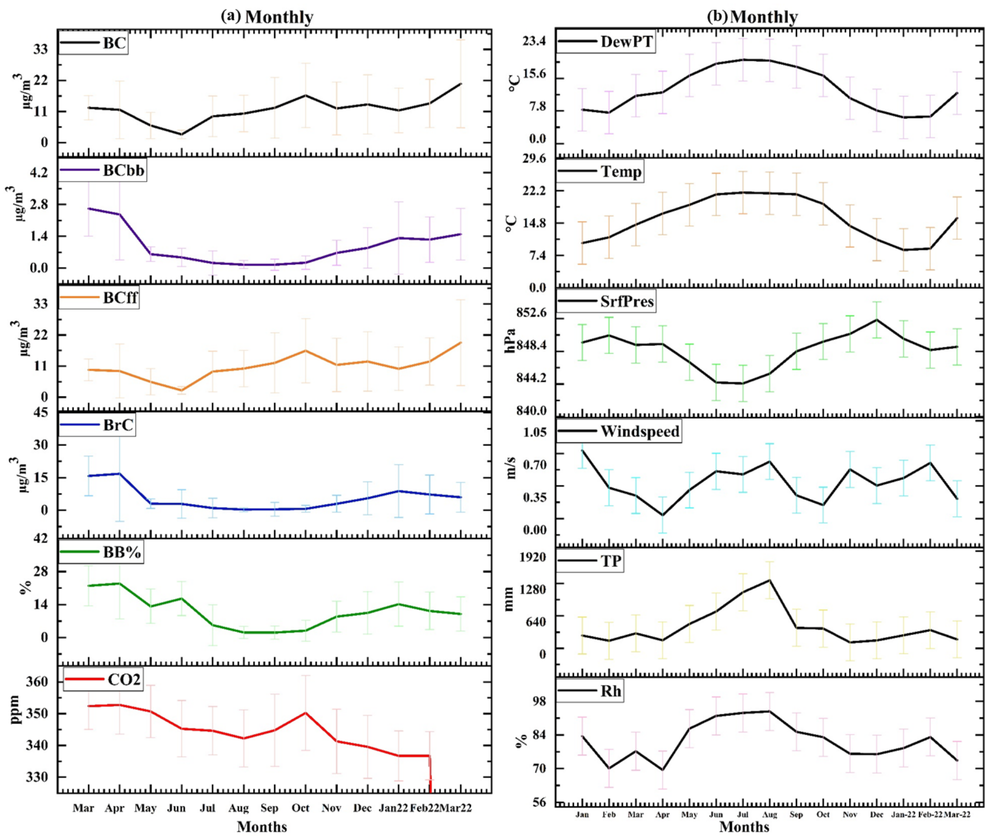


Figure 4. (a) The monthly mean of Black Carbon, Black Carbon through biomass burning, Black Carbon through fossil fuel, Brown Carbon, Biomass Burning percentage and Carbon Dioxide (BC, BCbb, BCff, BrC, BB%, and CO2, respectively) (The corresponding unit for BC, BCbb, BCff, BrC: µg/m3; BB%: % and CO2: ppm) for 16$^{th}$ March 2021 to 10$^{th}$ March 2022 over study location (lat:27.32; lon:88.61). The error bar shows ±σ standard deviation for each variable. (b) Same as figure 4a, but for meteorological parameters as dewpoint temperature (DewPT), temperature (Temp), surface pressure (SrfPres), windspeed, total precipitation (TP), and relative humidity (Rh) during January 2021 to March 2022.

https://doi.org/10.5194/egusphere-2023-702
Preprint. Discussion started: 4 October 2023


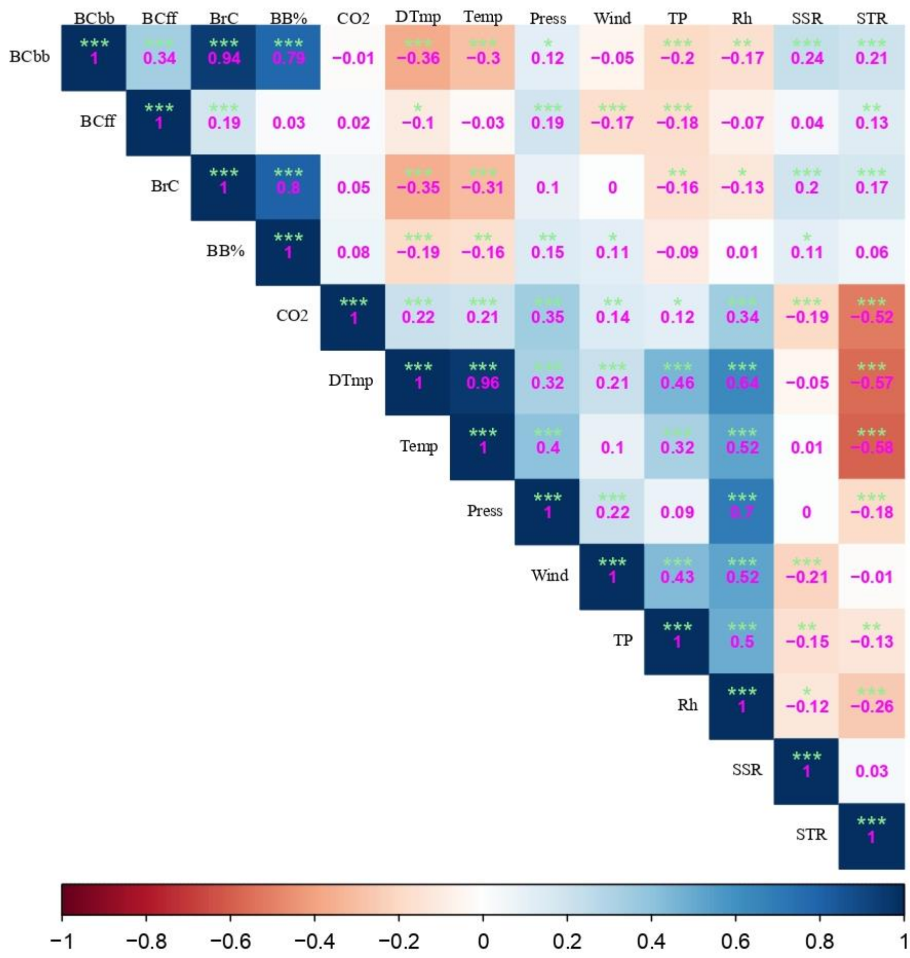


Figure 5. Correlation among BC, BCbb, BCff, BrC, BB%, $CO_2$ and, dewpoint temperature (DTmp), temperature (Temp), surface pressure (Press), Wind, total precipitation (TP), Relative humidity (Rh), net solar radiation (SSR), and net thermal radiation (STR). The (***) shows 99% significance, (**) shows 95% significance, (*) 90% significance and () shows no significance. The correlation coefficient values (-0.3 to -0.49) or (0.3 to 0.49) are considered as 'a good correlation', values ≤ (-0.5) or ≥ (0.5) considered as 'a strong correlation'.

https://doi.org/10.5194/egusphere-2023-702
Preprint. Discussion started: 4 October 2023


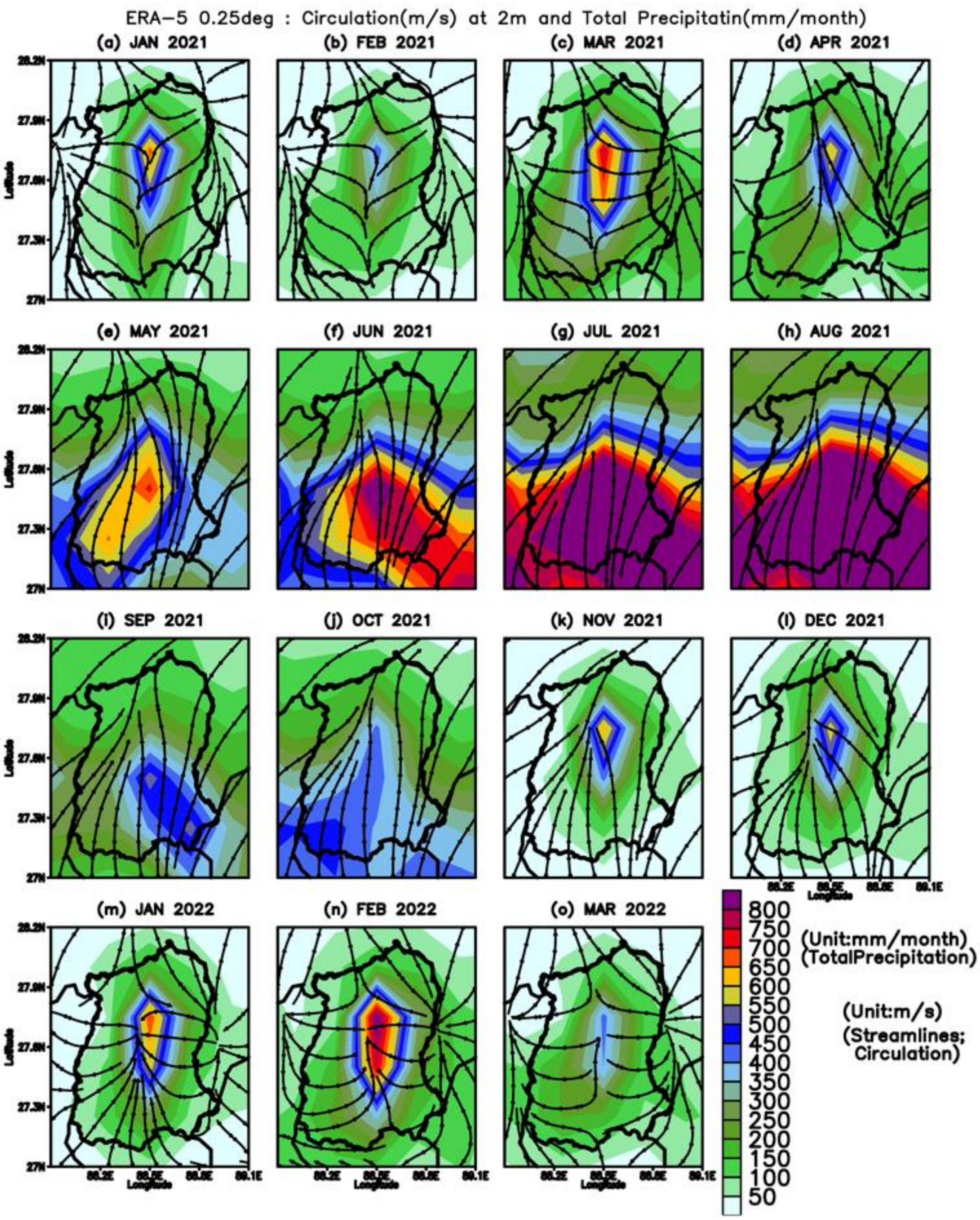


Figure 6. Monthly total precipitation (cumulative) and wind circulation pattern during January 2021 to March 2022. The Shading shows precipitation pattern, and streamline shows wind circulation.

https://doi.org/10.5194/egusphere-2023-702
Preprint. Discussion started: 4 October 2023


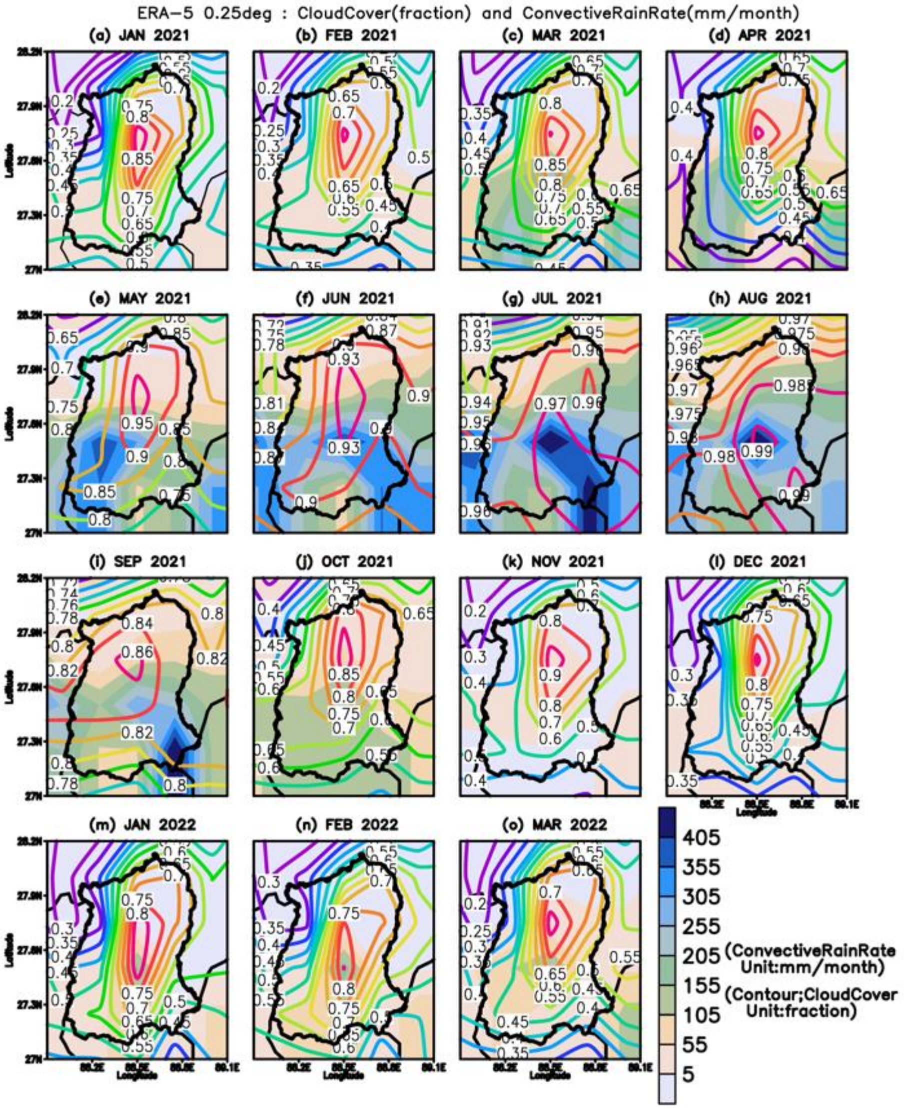


Figure 7. Monthly convective rain and total cloud cover during January 2021 to March 2022. The shading shows convective rain pattern, and contour shows total cloud cover fraction.

https://doi.org/10.5194/egusphere-2023-702
Preprint. Discussion started: 4 October 2023


**List of Tables**

Table 1. The details of datasets used for the present study.

| Variables | Data sets | Years (Span) | Resolution | | Source | Reference |
|---|---|---|---|---|---|---|
| | | | Temporal | Horizontal | | |
| Black and Brown Carbon | Observation and analysis, data generated using Aethalometer AE33 | March 2021- March 2022 | Weekly | Point Location (Gangtok) | Original data generated | Present Study |
| Total precipitation<br>Relative humidity<br>Temperature (2 meter)<br>Wind (surface wind)<br>Surface pressure<br>Dewpoint temperature<br>Net solar, and thermal radiation downward | ERA5 (ECMWF) | 2021 to 2022 | Hourly | 0.25º * 0.25º | ECMWF https://cds.climate.copernicus.eu/cdsapp#!/dataset/reanalysis-era5-single-levels?tab=form | Hersbach et al., 2020 |
| LULC | LandSat-5, LandSat-8 and earth explorer USGS | December 2000, December 2010, December 2020 | 2000, 2010, 2020 | 30m, 30m | earth explorer USGS. https://earthexplorer.usgs.gov/ | earth explorer USGS. |
| LULC | Sentinel-2 Esri Inc. | December 2021 | 2021 | 10 m | Esri Inc. https://www.arcgis.com/home/item.html?id=d3da5dd386d140cf93fc9ecbf8da5e31 | Karra et. al., 2021 |